Cassini Downlink Ka-Band Carrier Signal Analysis

David D. Morabito,* Daniel Kahan,* Kamal Oudrhiri,* and Carlyn-Ann Lee*

ABSTRACT. — Lower frequency telemetry bands are becoming more limited in bandwidth with more competition between flight projects and other entities. Higher frequency bands offer significantly more bandwidth and hence the prospect of much higher data rates. Future or prospective flight projects considering Ka-band (32-GHz) telemetry data links are interested in past flight experience with received Ka-band data. Over 10 years of Cassini closed-loop received Ka-band carrier data involving over 2 million individual measurements were acquired at all three Deep Space Network (DSN) sites. We analyzed these data to characterize link performance over a wide range of weather conditions and as a function of elevation angle. Based on this analysis, we have derived a recommendation for telecommunications link margin for preflight planning purposes. These results suggest that a 4-dB margin will ensure a ~94 percent data return at a minimum 20-deg elevation angle under 90 percent weather conditions at 32 GHz (Ka-band).

I. Introduction

Given that lower frequency telemetry bands are limited in bandwidth and becoming more competitive, flight projects are considering higher frequency bands offering significantly increased bandwidth and hence the prospect of using much higher data rates. Future or prospective flight projects that are considering Ka-band (32-GHz) telemetry data links are interested in examining past experience with received Ka-band data. Ka-band offers advantages such as more available bandwidth and a potential G/T (gain over system noise temperature ratio) advantage over lower frequency bands. Especially important to these flight projects is gaining an understanding of past flight experience due to weather effects from current or past missions flying Ka-band. This frequency band is more susceptible to weather effects than lower frequency bands currently used for most standard downlink telemetry.

We analyzed received signal measurements from the Deep Space Network (DSN) closed-loop receivers in order to assess performance degradations due to weather. The data sets from 2004 to 2015 were acquired during science investigations and calibrations conducted by the Cassini Radio Science Team where the spacecraft was in orbit around the planet Saturn.

* Communications Architectures and Research Section.

The research described in this publication was carried out by the Jet Propulsion Laboratory, California Institute of Technology, under a contract with the National Aeronautics and Space Administration.

These data included carrier-to-noise density ratio (P_c/N_0) measurements received at beam-waveguide (BWG) antennas at all three DSN sites at Goldstone, California; Madrid. Spain; and Canberra, Australia, as well as operating system noise temperature (T_{op}). In addition, ancillary data were made use of in this analysis and included water vapor radiometer (WVR) data and surface meteorological data. In this article, we discuss the behavior of the closed-loop receiver P_c/N_0 measurements with time, with elevation angle, and with respect to tracking site, as well as with any seasonal weather patterns. Higher temporal resolution data from the DSN open-loop receivers were also acquired but the analysis involving these data will be the subject of future study.

The primary purpose of this study is to provide future and prospective missions desiring to use Ka-band a set of recommendations with regard to margin policy based on the study's findings. In the preflight stages of a flight program, telecommunications links are usually designed with a 3 dB (or higher) margin above a threshold based on "worst-case" or "conservative" assumptions. Such conservative link assumptions include farthest range distance, lowest elevation angle during a pass, and a high percentage weather availability. The weather availability assumptions for the threshold typically involve a 90 percent cumulative distribution of atmospheric attenuation and atmospheric noise temperature. These statistics (atmospheric attenuation and atmospheric noise temperature) are well documented for the DSN and based on decades of water vapor radiometer (WVR) 31.4-GHz sky brightness temperature [1]. DSN engineers employ appropriate models from [1] to adjust the statistics of WVR data to the frequency bands used by the DSN: 2.3 GHz (S-band), 8.4 GHz (X-band), 26 GHz (K-band), and 32 GHz (Ka-band). In this article, we will focus on the 32-GHz (Ka-band) deep-space allocation.

Telecommunications teams make use of separate (but coupled) link budgets for carrier, telemetry channel, and ranging channel, each having their own set of assumptions. In order to simplify the discussion, we will assume the case of no-ranging. The carrier channel threshold involves maintaining a minimum carrier tracking loop signal-to-noise ratio (SNR) required to maintain lock. The *DSN Telecommunications Link Design Handbook*, DSN No. 810-005 [2] provides recommendations for minimum SNR for different link configurations. For residual carrier tracking involving binary phase-shift keying (BPSK) telemetry, a minimum loop-SNR of 10 dB is required, whereas for suppressed-carrier BPSK, it is 17 dB [2]. There are higher threshold carrier loop-SNR values required for quadrature phase-shift keying (QPSK) telemetry. The carrier link also takes into account transmitter phase noise and solar phase noise (significant at small solar elongation angles). Usually projects maintain a carrier link with 3 dB or higher margin above the SNR threshold.

The telemetry channel (or data channel) threshold is typically characterized by the energy per bit to noise power spectral density ratio (E_b/N_0) that yields a maximum frame-error rate (FER) or bit-error rate (BER). Thus, a telemetry channel threshold E_b/N_0 will have a dependence on the threshold BER/FER desired and the applicable coding scheme [2]. A typical link budget for a planetary orbiter may involve designing a data channel link with at least 3 dB margin above threshold.

In cases where a residual carrier is employed, the distribution of power between carrier channel and data channel is based on a modulation index that is suitably chosen. For the

case of suppressed carrier operations, we can think of the carrier as being a "reconstructed" carrier obtained during ground processing. A lander or probe telecommunication link may use a higher margin depending upon link parameter uncertainties.

NASA space missions make use of link budget analysis using design control tables (DCTs). These tables include numerous parameters dealing with the transmitter, channel and receiver of the telecommunications system [3,4]. The margin policy used in the link budgets is based on well-established guidelines. The flight experience with X-band during prelaunch planning phases has been to use standard 3-dB margins above a conservative threshold when there are nominal uncertainties with the link (such as with orbiters), and about 6 dB or 10 dB for links with higher uncertainties such as with landers or entry probes. As the uncertainties are reduced or "trimmed down," the required margins become lower.

During the operations phase of a mission, the standard link margin can reach down to 2 dB or even lower. For instance, projects typically make use of "mean minus 3-sigma" margins for commanding and "mean minus 2-sigma" for their downlink telemetry, such as for Voyager in early stages of that mission [5]. However, in recent years, as the Voyager spacecraft become more distant (137 AU as of December 2016), maintaining the link has become more challenging. As the signal has become much weaker, multiple antennas are arrayed together to increase ground G/T. In addition, the minimum elevation angle for a tracking pass has increased gradually each year, and the link operated at threshold based on optimistic weather condition assumptions.[1] In this case, the Voyager project accepts a degree of occasional data loss due to bad frames.

For the case of the Mars Exploration Rovers at X-band, the "mean minus 2-sigma" downlink criterion turned out to be overly optimistic while on the Martian surface, as this meant that there was only about ~1 dB of margin to account for any variations in performance such as due to weather [6]. In cases where the project could not accept virtually any data loss, a judicious selection of data rate was uplinked to the spacecraft prior to a tracking pass [6].

The Kepler spacecraft, in an Earth-trailing orbit, makes use of a Ka-band telecommunications system for downlink. The basic approach was to design links with 3 dB margin;[2] however, early in the mission, significantly higher margins were realized using the highest available downlink rate. As the spacecraft distance has increased, the available margin has decreased. A recent study [7] reported on the analysis of one year of Kepler flight data from 2012. This study focused on how operational data may differ from expected behavior and attempted to quantify variations in received signal power such as due to winds, clouds, and rain. Understanding such variations is important to future missions, especially those that operate at low margins. Possible considerations that may influence the margin policy may depend on whether a project opts to make use of weather forecasting to set their data rates prior to a tracking pass [8].

---

[1] Roger Ludwig, JPL, personal communication, December 13, 2016.

[2] Wayne Davis and Rebecca Walter, *Spacecraft Telecommunications Subsystem Design Data Book*, Ball Aerospace (internal document), March 22, 2005.

Given that the weather effects at Ka-band are significantly greater than those at X-band, the existing margin policy (typically used for X-band) needs to be revisited and possibly revised. This can also depend upon the requirements of a given mission.

The purpose of the present article is to closely examine or review the Cassini flight experience with carrier-only Ka-band and provide a recommended margin policy for future missions wishing to fly a Ka-band telecommunications system. We first describe the observations used in this study in Section II. We then examine the averaged P_c/N_0 over each tracking pass in Section III. We next examine the individual closed-loop P_c/N_0 measurements in Section IV. Finally, we provide baseline recommendations on margin policy in Section V, followed by concluding remarks in Section VI.

II. Observations

The Cassini spacecraft launched from Earth on October 15, 1997, and executed gravity assists with Venus on April 26, 1998, Venus again on June 24, 1999, Earth on August 18, 1999, and Jupiter on December 30, 2000, sending it on a trajectory toward Saturn. The spacecraft arrived at Saturn on July 1, 2004, when it went into orbit and began a four-year primary mission of exploration of Saturn and its environment. Since then, there have been several extensions of the primary mission. The radio science experiments on board Cassini made use of the X- (8.4-GHz), S- (2.3-GHz), and Ka- (32-GHz) downlink carrier links. A description of the radio science experiments is available in [9]. The Cassini mission will terminate in September 2017, when the spacecraft will be plunged into the atmosphere of Saturn while taking final in situ measurements.[3]

The Cassini spacecraft has a 4-m-diameter high-gain antenna (HGA) used to simultaneously transmit (as well as receive) the X-band and Ka-band signals to (from) Earth. The spacecraft transmitter power assumed for the link budgets is 7.1 W at Ka-band. The link budget parameters for the spacecraft assume 1.7 dB of circuit loss and 1.53 dB of pointing loss. The Cassini radio science experiments typically make use of reaction wheels, which result in little or no pointing loss. The passes where thrusters were required for coarse pointing control (several dB pointing loss), were not included in the data set for this study. For normal communications, including radio science observations, the HGA is pointed directly at Earth, but at times, for observations conducted by other instruments, the spacecraft may rotate about its –Z axis. Because the –Z axis is close but not perfectly aligned with the HGA, the pointing of the antenna oscillates on and off Earth-point, causing a sinusoidal pattern (on the order of a few dB) in the signal strength received at Earth. These periodic pointing loss signatures due to spacecraft rolling and Earth line-of-sight misalignment with the HGA involve excursions of ~2 dB in signal strength, and these were retained in the analyzed data as they are understood to lie within acceptable limits. Detailed descriptions of preflight link budget assumptions and parameters for Cassini are available elsewhere.[4]

---

[3] https://saturn.jpl.nasa.gov/mission/grand-finale/overview/

[4] A. Makovsky, *Cassini Telecommunications Link Design Control Document*, PD 699-257/JPL D-14189 (internal document), Jet Propulsion Laboratory, Pasadena, California, July 29, 1996.

The ground antennas used to receive the Ka-band signal were 34-m-diameter beam-waveguide (BWG) antennas that usually employed monopulse tracking for pointing control. The ground antenna parameters utilized in the link budget analysis included those needed for antenna gain and ground system noise temperature (SNT) contributions and were extracted from [10].

The DSN closed-loop receivers were configured to output carrier signal strength and frequency at 1 s temporal resolution. The primary data type examined for this study was carrier-to-noise density ratio (P_c/N_0). The spacecraft was configured to transmit either a carrier referenced to the onboard oscillator (an ultrastable oscillator until 2011, and auxiliary oscillator after 2011) for one-way mode, or coherent X-band uplink transmitted to the spacecraft from the same (two-way) or different (three-way) ground station employing very stable frequency references (hydrogen maser frequency standards).

There were ~250 tracking passes involving a Ka-band downlink conducted between 2004 and 2015 using 34-m-diameter BWG ground stations. Figure 1 displays the range distance between Cassini and Earth between 2004 and 2017, including the period of data acquisition. The minimum range distance encountered during the observations (2004–2015) was ~8 AU and the maximum was ~11 AU, resulting in a ~3 dB difference between these two extremes in the space loss contribution of signal power in the link budgets. The examination of the closed-loop P_c/N_0 measurements also included comparison with favorable and adverse link curves. We chose not to adjust the P_c/N_0 observations to a common range distance in order to retain the purity of the measurements in the study. We instead adopted the convention that the favorable link curve be based on the minimum range distance encountered during the observation set (along with other favorable assumptions), while the

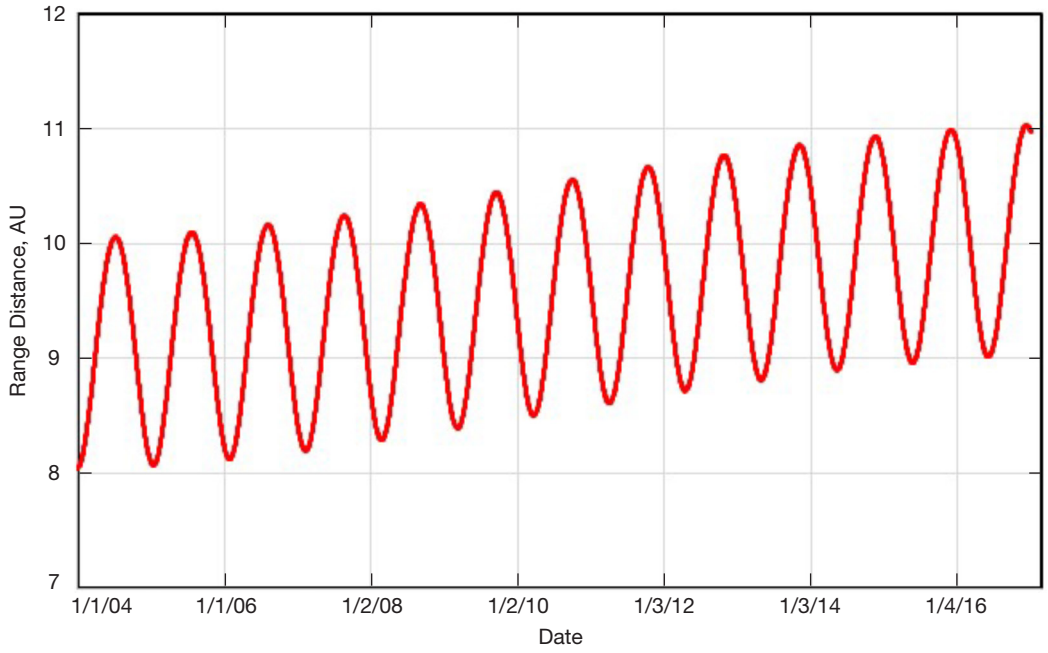

Figure 1. Range distance between Cassini spacecraft (in orbit around Saturn) and Earth between January 1, 2004, to December 31, 2017.

adverse curve includes the space loss based on the maximum range distance encountered during the observations (along with other conservative assumptions). Inspecting data lying below the adverse link curve allowed us to more readily identify candidate data sets degraded by nonatmospheric influences, such as equipment issues, significant loss due to antenna mispointing, or unanticipated charged-particle effects.

Figure 2 depicts the minimum solar elongation angle as a function of time during the period of the Cassini radio science data discussed here. Since the higher frequency Ka-band is less susceptible to solar scintillation effects than X-band (where telemetry becomes significantly degraded at ~3 deg), one should be able to probe down to lower Sun–Earth–probe (SEP) angles (~1 deg) before telemetry is expected to be significantly degraded [11]. However, amplitude scintillation effects can be significant at Ka-band below 3 deg SEP angle (depending upon solar coronal conditions and activity). Thus, measurements that occur at SEP angles of 3 deg and below have been filtered out of the one-way observations in order to better characterize atmospheric (and other) effects. During this study, significant "scatter" was found to be present in many of the coherent Ka-band measurements at SEP angles above 3 deg. This increased scatter of the two-way measurements at Ka-band is attributed to coronal-induced phase fluctuations on the X-band uplink that are multiplied by the spacecraft transponder, which translate them to the downlink Ka-band carrier. This additional degradation on the coherent downlink Ka-band carrier necessitated using a higher SEP cutoff of up to 6 deg.

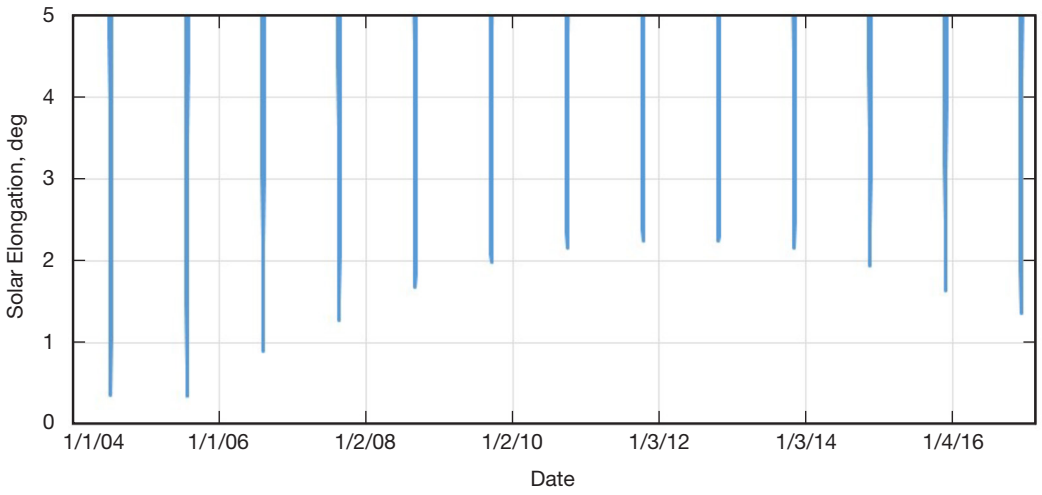

Figure 2. Solar elongation angle (less than 5 deg) versus time for the period of Cassini data discussed in this article. "End-points" denote minimum SEP angle for each solar superior conjunction period.

III. Closed-Loop Data Analysis — Average P_c/N_0 Over a Tracking Pass

We first examine the closed-loop data from all three DSN sites in terms of averaged P_c/N_0. Roughly 250 downlink passes were conducted between 2004 and 2015 involving 34-m-diameter BWG ground stations. Figure 3 displays the averaged P_c/N_0 for each pass versus date of experiment and Figure 4 displays average P_c/N_0 versus the average elevation angle over each pass. Different color filled-circles in Figures 3 and 4 denote the average P_c/N_0 for

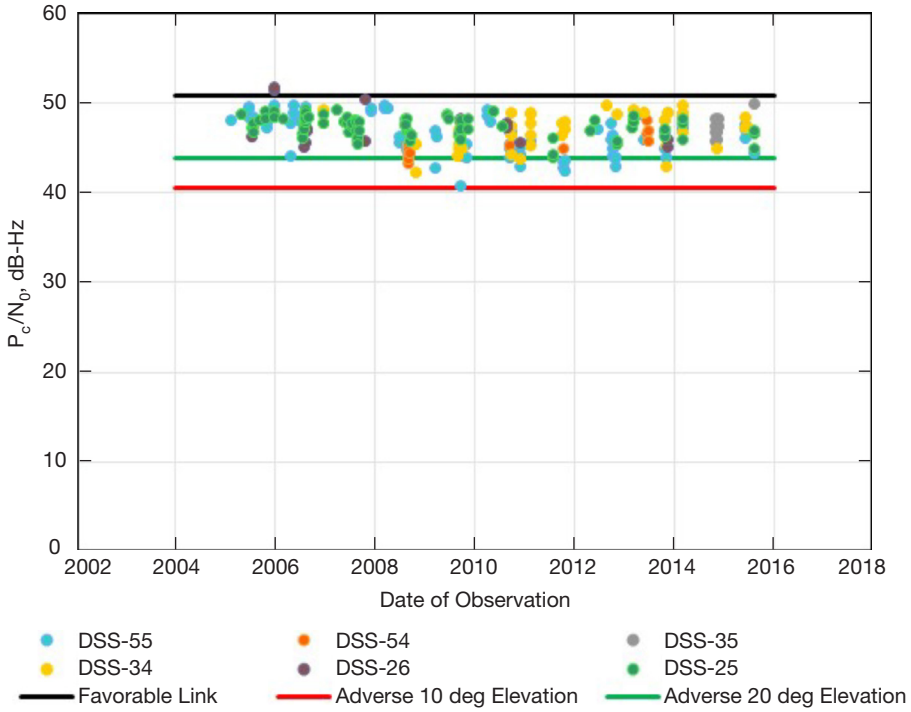

Figure 3. Average P_c/N_0 versus experiment date for each tracking pass along with favorable curve (90 deg elevation) and adverse curves (10 deg and 20 deg elevation). Each data point is color-coded to represent a particular 34-m-diameter DSN ground antenna (see legend).

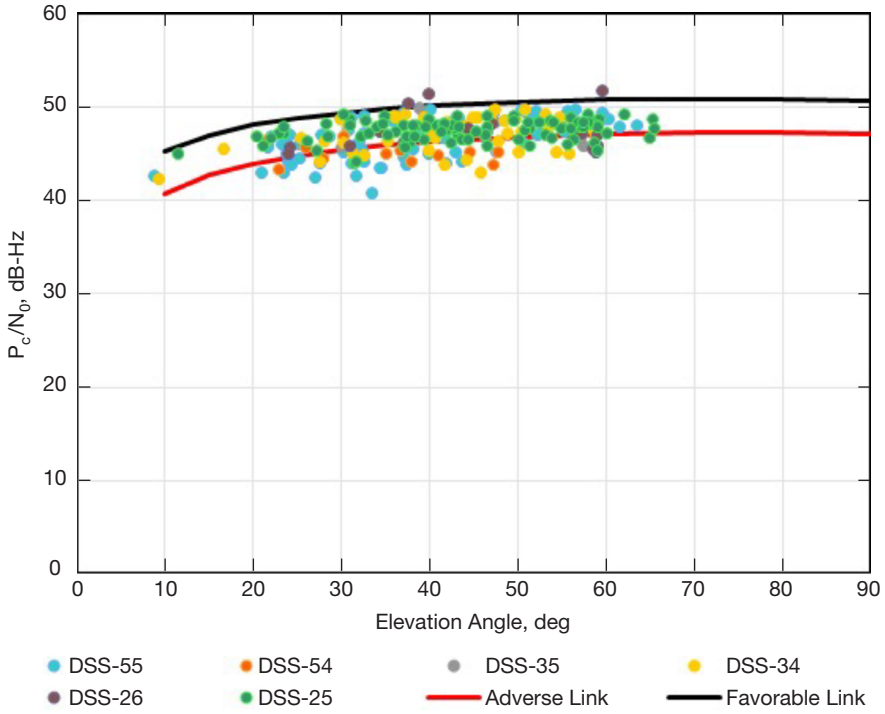

Figure 4. Average P_c/N_0 versus average elevation angle over each tracking pass along with favorable (black) and adverse (red) threshold curves. Each data point is color coded for a particular 34-m-diameter DSN antenna (see legend).

each antenna pass. Also shown on these plots are the favorable (black) and adverse (red and green) link curves, based on the link budget analysis. The favorable link assumed the closest range distance between Earth and Saturn (8.25 AU), and favorable weather conditions (50 percent availability) based on the best weather site (Goldstone) using the atmospheric attenuation and atmospheric noise temperature statistical tables found in [1]. The adverse link assumed the farthest range distance between Earth and Saturn (10.99 AU), and pessimistic weather conditions (90 percent availability) based on the site with the most adverse weather (Canberra). The link budget parameters for the spacecraft transmit power, HGA, circuit loss, and pointing loss made use of Cassini telecommunications design parameters as described in Section II.

The favorable link curves presented in Figures 3 and 4 do a good job in bounding the upper envelope of the P_c/N_0 averages. The adverse link curves shown in Figure 3 pertain to both 10 deg (red) and 20 deg (green) elevation angle cases. The favorable (90 deg elevation) and adverse (10 deg elevation) link curves envelop virtually all the data points in Figure 3. The adverse link curve as a function of elevation angle shown in Figure 4 has several data points that lie below it. However, the majority of the average value P_c/N_0 measurements lie between the two curves. We see that a 4- or 5-dB margin below the adverse link curve in Figure 4 will contain virtually all of the average P_c/N_0 measurements. Some of the average P_c/N_0 passes include periods of degraded data due to atmospheric effects and pointing issues, and thus an examination of all individual measurements is required and is the focus of discussion in Section IV.

Figure 5 depicts the average P_c/N_0 measurements versus elevation angle for the Goldstone-only passes, where the favorable and adverse link curves are based on the above-stated assumptions but pertaining to Goldstone weather and station configurations. Here we see

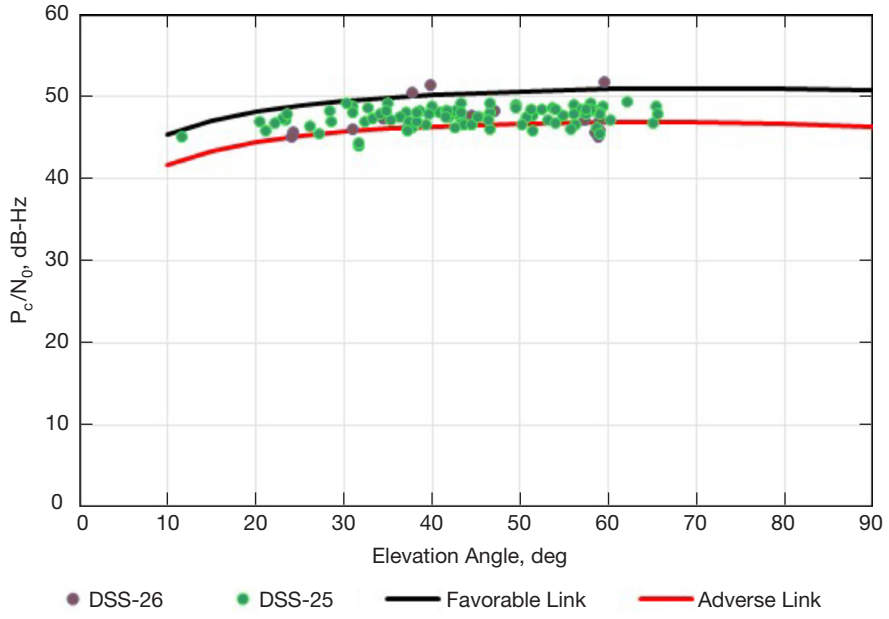

Figure 5. Average P_c/N_0 versus average elevation angle over each Goldstone tracking pass along with favorable (black) and adverse (red) curves. Each data point is color coded for a particular 34-m-diameter DSN antenna (see legend).

that a 2-dB margin below the adverse curve covers all average P_c/N_0 measurements. Again, we need to examine the individual point measurements in order to make a more informed quantitative statement on margin policy (see Section IV).

Figure 6 depicts the average P_c/N_0 measurements versus elevation angle for the Madrid-only passes, where the favorable and adverse link curves are based on the above stated assumptions but pertaining to Madrid weather and station configurations. Here we see that a 5-dB margin below the adverse curve covers almost all measurements. Again, we need to examine individual point measurements in order to make a more informed quantitative statement on margin policy (see Section IV).

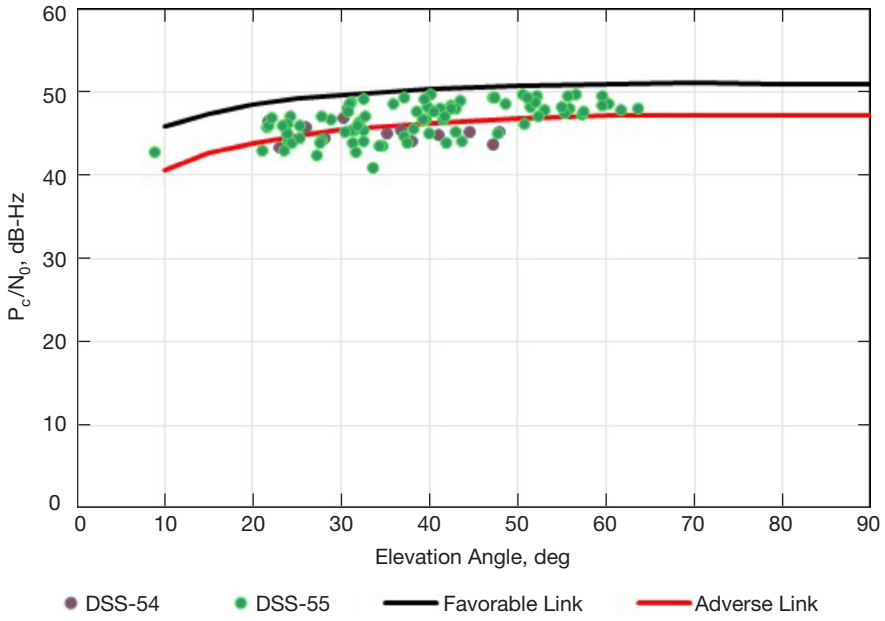

Figure 6. Average P_c/N_0 versus average elevation angle over each Madrid tracking pass along with favorable (black) and adverse (red) curves. Each data point is color coded for a particular 34-m-diameter DSN antenna (see legend).

Figure 7 depicts the average P_c/N_0 measurements versus elevation angle for the Canberra-only passes, where the favorable and adverse link curves are based on the above-stated assumptions but pertaining to Canberra weather and station configurations. Here we see that a 4-dB margin below the adverse curve covers all average P_c/N_0 measurements. Again, we need to examine the individual point measurements in order to make a more informed quantitative statement on margin policy (see Section IV).

To achieve a better understanding of the behavior of the data and to disentangle weather effects from other sources of degradation, it is necessary to examine the received P_c/N_0 for each receive antenna on an individual data point by data point basis, as will be discussed in the next section.

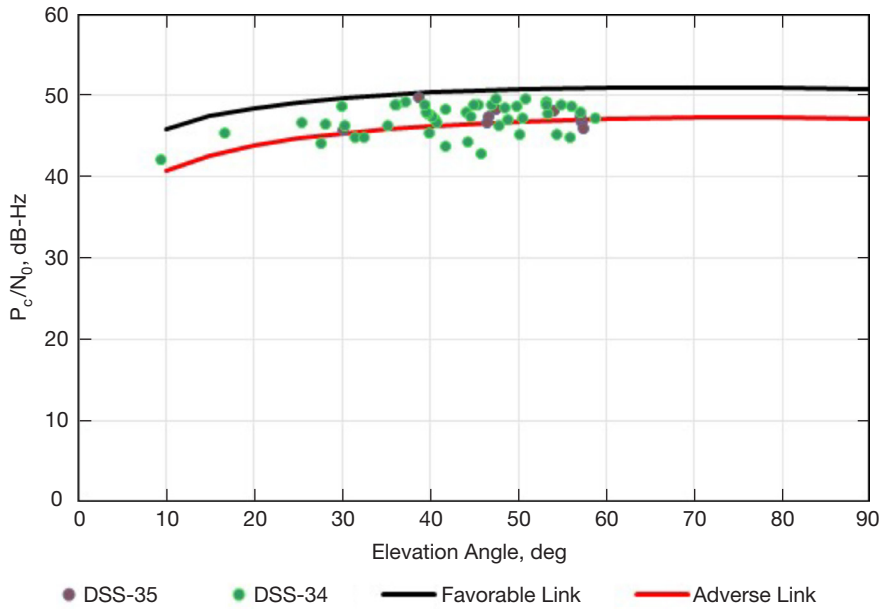

Figure 7. Average P_c/N_0 versus average elevation angle over each Canberra tracking pass along with favorable (black) and adverse (red) link curves. Each data point is color coded for a particular 34-m-diameter DSN antenna (see legend).

IV. Closed-Loop Data Analysis — Individual P_c/N_0 Measurements

We next examine the P_c/N_0 versus elevation angle behavior of all of the individual measurements for each 34-m BWG antenna at each of the three DSN tracking sites and tracking modes. The closed-loop receivers sampled the individual P_c/N_0 measurements at a 1/s rate. Thus, a 1-hr period would consist of 3600 individual measurements, and an 8-hr pass would include up to 28800 data points. Thus, over the course of the 2004–2015 data span, we acquired over two million individual Ka-band P_c/N_0 measurements from all Ka-band–capable DSN antennas.

A. Goldstone, California

Figure 8 depicts the P_c/N_0 versus elevation angle signature of the individual 1-s data points (small blue dots)[5] from the Goldstone passes involving the DSS-25 34-m BWG antenna for all three tracking modes (one-way, two-way, and three-way). Also shown are the favorable and adverse link curves. It is noteworthy that the favorable link curve (black) effectively "hugs" the upper envelope of the P_c/N_0 measurements, thus providing confidence in the link budget assumptions. The link budget curves could vary up or down to about ~1 dB due to uncertainties in some of the link parameters. The P_c/N_0 data plotted in Figure 8 contain about 587434 data points, that were "filtered" out from ~900000 data points where solar conjunction passes were removed, low-amplitude points (during signal acquisition, mode changes, and end-of-track loss-of-signal periods) were removed, and cases that involved

[5] In this article, very small symbols are used for P_c/N_0 and SNT in order to maintain a clear view of the signatures and envelopes of the data since there are well over 100,000 data points in many cases, and larger symbols would tend to "smear" out many features seen in the plots.

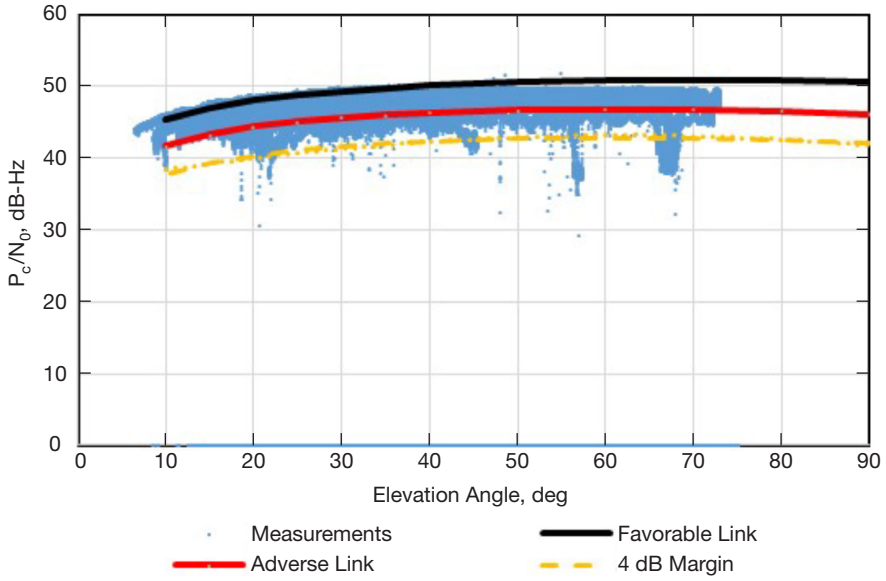

Figure 8. Received P_c/N_0 (blue data points) versus elevation angle for DSS-25 with adverse (red), favorable link (black), and 4-dB margin (dashed yellow) curves.

"egregious" mispointing were removed. Some of the data points lying below the adverse curve could still be subject to mispointing. However, a 4-dB margin below the adverse curve virtually covers all the sampled data. We believe that the vast majority of data lying below the 4-dB margin curve is attributable to weather.

Figure 9 depicts the P_c/N_0 versus elevation angle signature of the individual 1-s data points from the Goldstone passes involving the DSS-26 34-m beam-waveguide antenna, along with favorable and adverse link curves. The P_c/N_0 data plotted in Figure 9 contain about 143488 data points, and were filtered out from ~230000 data points. The data were filtered

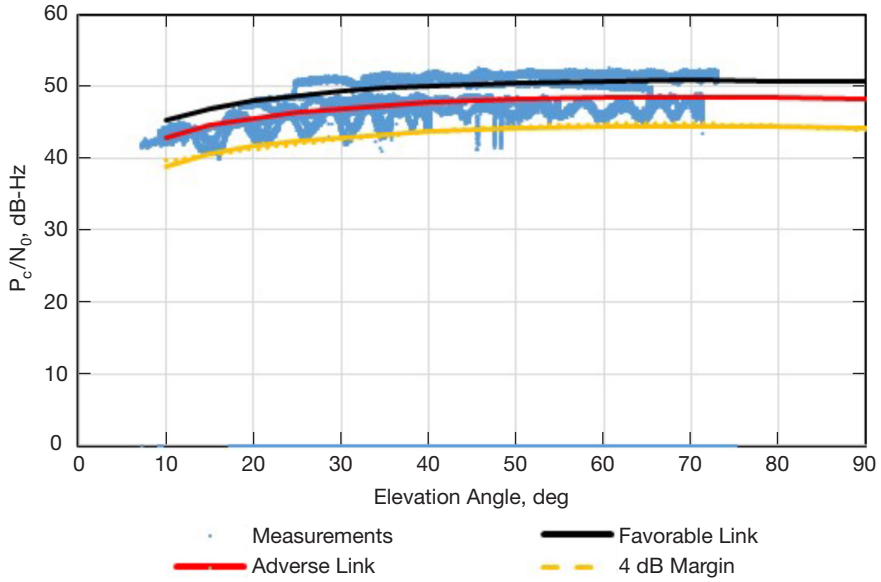

Figure 9. Received P_c/N_0 (blue data points) versus elevation angle for DSS-26 with adverse (red), favorable link (black), and 4-dB margin (dashed yellow) curves.

in the same manner as that described for DSS-25 (Figure 8). We note that from inspection of Figure 9, most of the DSS-26 data lie below the favorable link curve. Almost all the data lie above the adverse link curve except for the data shown by the sinusoidal-like signature. There were fewer passes involving DSS-26, and thus one can more easily inspect the periodic variation of the P_c/N_0 from individual passes in Figure 9. The peaks of the sinusoidal-like signature appear to lie on or above the adverse link curve, and the "dips" lie above or on the 4-dB margin curve. The peaks likely occur when the spacecraft antenna is closer to Earth-point. The data below the peaks of the sinusoidal-like signature is off-pointed and attributed to the rolling motion of the spacecraft during this mode. Most of the data lying below the 4-dB curve is believed to be attributable to atmospheric degradation.

Figure 10 illustrates an example of a DSS-25 pass degraded by atmospheric effects, which displays P_c/N_0 (blue points) versus time for data acquired on December 27, 2006. The large signal fades such as those near 12:00 UTC are anti-correlated with large increases in SNT (although noisy), consistent with increased atmospheric effects at Ka-band.

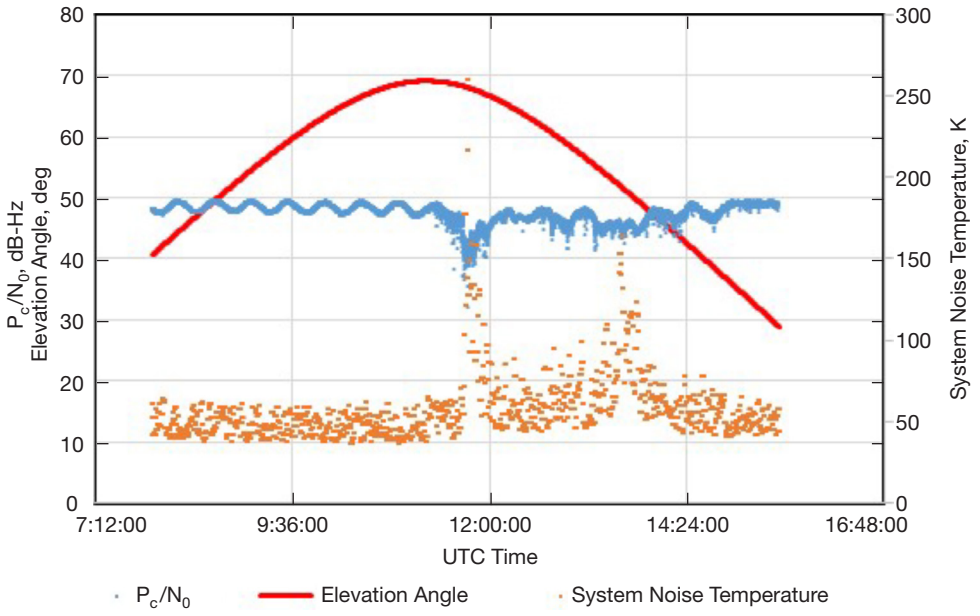

Figure 10. Example of atmospheric degradation in P_c/N_0 data (blue points) acquired during the DSS-25 pass conducted on December 27, 2006. Also shown are elevation angle profile (red curve) and system noise temperature (SNT) (brown points).

B. Madrid, Spain

Figure 11 displays the individual P_c/N_0 data points versus elevation angle for Madrid DSS-55 when tracking Cassini's Ka-band carrier. The favorable link curve assumes the minimum range distance between Earth and Cassini, favorable weather, and lowest noise ground configuration. It is noteworthy that the favorable link curve bounds the upper envelope of the P_c/N_0 measurements, thus providing a degree of confidence in the consistency of the link budget assumptions. The P_c/N_0 data plotted in Figure 11 consist of 696418 data points. These data were filtered from ~900000 original data points in the same manner as that described for DSS-25 (Figure 8). The adverse link curve assumes the maximum range distance between Earth and Cassini, 90 percent weather as well as the highest noise ground

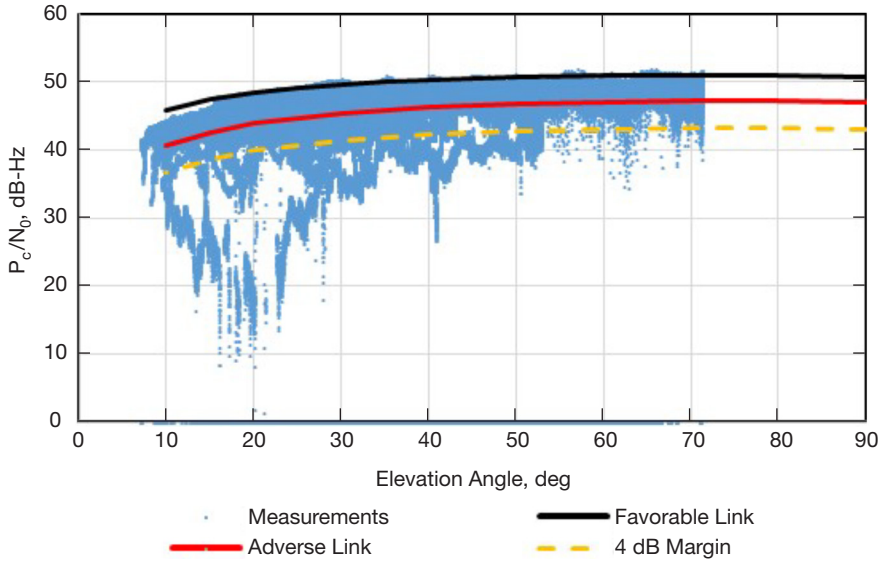

Figure 11. Received P_c/N_0 versus elevation angle for DSS-55 (blue points) with adverse (red) and favorable (black) link curves. Also plotted is the 4-dB margin (relative to adverse) (dashed yellow).

configuration. The dashed yellow curve displays the 4 dB below the adverse curve. There are a significant number of data points that lie below the 4-dB margin curve, most of which appear to exhibit classic "rain fade" behavior.

We desire to make a close examination for the two individual passes showing the most significant rain fade signatures in Figure 11. The individual P_c/N_0 time signatures for these two passes occurring on October 27, 2011, and November 4, 2012, are shown in Figure 12(a) and Figure 13(a), respectively. The P_c/N_0 fades seen during these two passes definitely appear to be anti-correlated with SNT, thus providing evidence that these fades are likely atmospheric in nature. An examination of Advanced Water Vapor Radiometer (AWVR) zenith 31.4-GHz sky brightness temperature data for October 27, 2011, further corroborates this [see Figure 12(a) green circles]. The SNT and AWVR data are not expected to necessarily align, as the AWVR sky brightness is referenced to zenith while the tracking antenna SNT measurements are representative measurements taken by the station at the elevation angles of the P_c/N_0 observations. The SNT measurements for October 27, 2011 [Figure 12(a)] and November 4, 2012 [Figure 13(a)] also include contributions due to ground station equipment. The SNT measurements were converted to estimates of atmospheric "fades" using models provided in [1]. The resulting signal level variations were referenced to estimates of P_c/N_0 using appropriate link budget adjustments [see Figure 12(b]. These estimates of P_c/N_0 (green) agree very well with the measured P_c/N_0 measurements (blue and purple), thus providing evidence that the observed variations are indeed atmospheric in nature and not due to other effects (such as variations in antenna pointing).

DSS-55 was tracking Cassini at very low elevation angles at the start of the tracks, thus the signal fades are of much larger magnitude than they would be at higher elevation angles. If we adjust the October 27, 2011, AWVR sky brightness temperatures for elevation angle and frequency, they more closely match the SNT measurements, but not exactly since the two instruments were sensing different directions in the sky during the turbulent conditions.

(a)

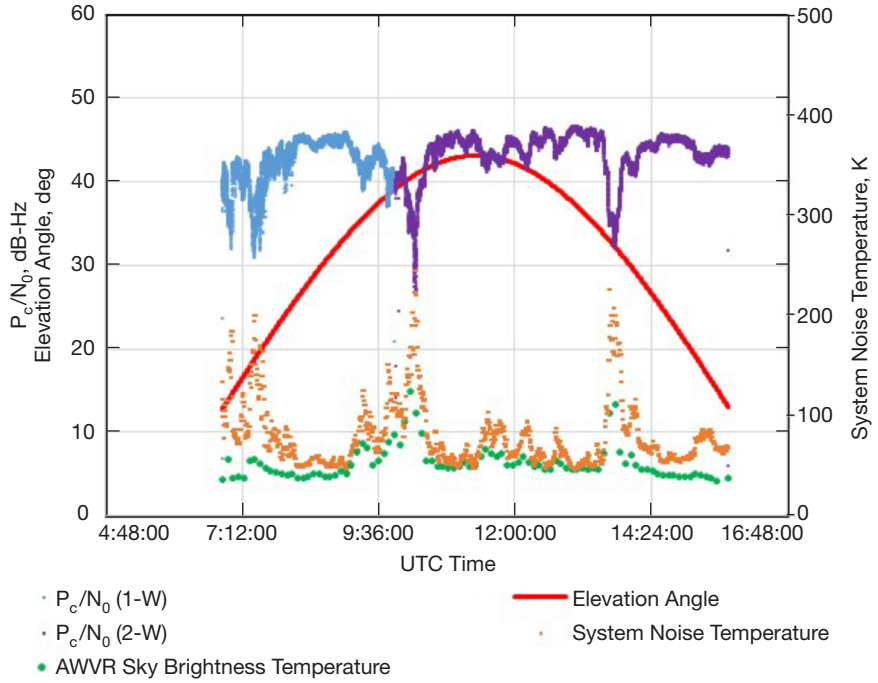

(b)

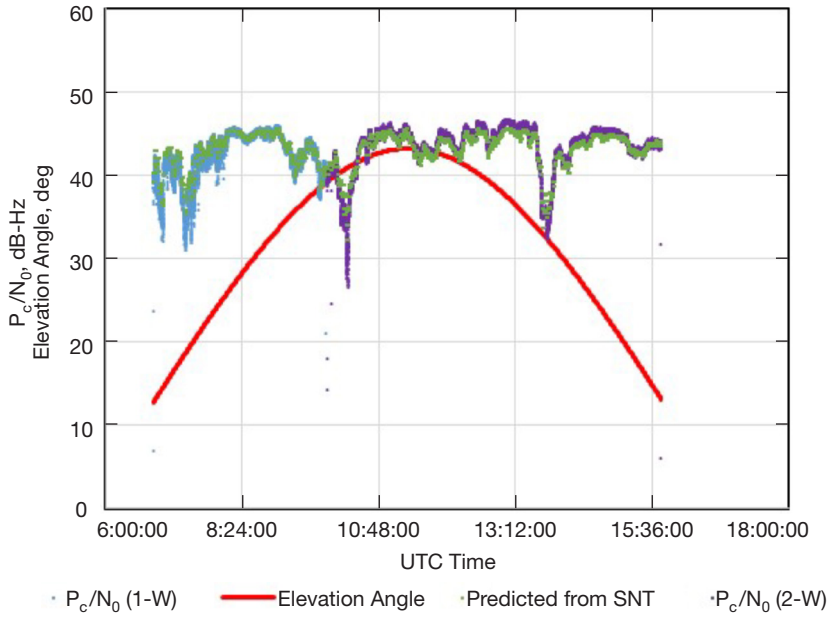

Figure 12. (a) Times series for one-way P_c/N_0 (blue), two-way P_c/N_0 (purple), SNT (brown), AWVR 31.4-GHz sky brightness temperature (green), and elevation angle (red curve) for DSS-55 tracking pass conducted on October 27, 2011; (b) times series for one-way P_c/N_0 (blue), two-way P_c/N_0 (purple), P_c/N_0 predicted from SNT (green), and elevation angle (red curve) for tracking pass depicted in (a).

(a)

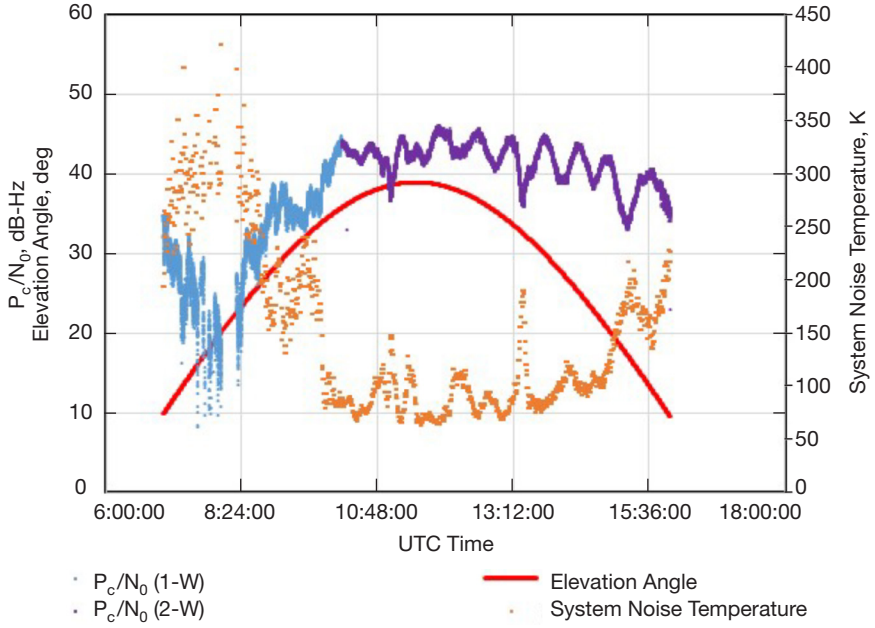

(b)

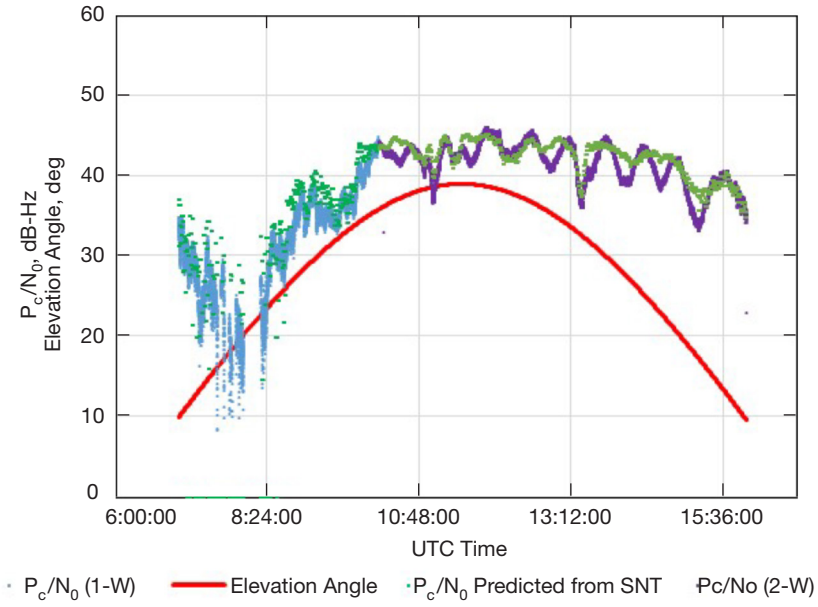

Figure 13. (a) Times series for one-way P_c/N_0 (blue), two-way P_c/N_0 (purple), SNT (brown), and elevation angle (red curve) for DSS-55 tracking pass conducted on November 4, 2012; (b) times series for one-way P_c/N_0 (blue), two-way P_c/N_0 (purple), P_c/N_0 predicted from SNT (green), and elevation angle (red curve) for tracking pass depicted in (a).

In any event, the AWVR and SNT data (along with surface meteorological data taken at the site) provide evidence that the P_c/N_0 degradations were due to weather.

Huge signal fades were observed at low elevation angles during the start of the November 4, 2012, tracking pass [see Figure 13(a)]. As there were no AWVR data available for November 4, 2012, due to equipment issues, we had to rely solely on the SNT data to infer atmospheric effects. However, nearby rain gauge data confirm significant rainfall during this pass, and thus significant liquid water along the signal path. The atmospheric noise temperature inferred from the SNT measurements (brown points) exceeds the 99 percent availability due to weather for a significant fraction of the track. Thus, this pass is representative of a less than 1 percent of the time occurrence. During this pass, a few SNT measurements were in excess of 400 K [see Figure 13(a)], and are attributable to noisier conditions during the rain.

During the one-way period at the start of this pass [see Figure 13(b)], the P_c/N_0 estimates (green) from the SNT data appear to reasonably track the large excursions in the measured P_c/N_0 (blue). The excursions here are largely attributable to weather. During the less noisy two-way period, the estimated P_c/N_0 (green) appear to overlay well with some measured P_c/N_0 (purple) variations, but not all, especially during the troughs, which appear periodic in nature. Thus, in this case, the excursions between measurements and estimates are mostly due to pointing caused by the rolling motion of the spacecraft. The predicted P_c/N_0 are in better agreement with the peaks in the measured P_c/N_0, as the variations are generally not large enough to coincide with most of the troughs.

If we remove from the P_c/N_0 data shown in Figure 11 for these two significant "rain" event passes depicted in Figures 12 and 13, we find that almost all of the remaining data points lie above the 4-dB margin curve. Given that the data from the October 27, 2011, and November 4, 2012, passes in Figure 11 constitute about 7 percent of the total data in this sample, these two passes would be expected to constitute a lower percentile level if one were able to sample P_c/N_0 as often as WVR data were collected [1]. We believe that 4 dB may be a reasonable recommended margin above a threshold based on 90 percent weather for use in Madrid link budgets (to be discussed in Section V).

The data shown in Figure 11 represent data taken at range distances between maximum and minimum possible during the several-year period and not normalized to a standard range distance. It is preferred that the P_c/N_0 data shown in the figures be the raw measurements. Thus, we choose to define the link curves appropriately for bounding purposes with favorable and adverse link assumptions for discerning margin policy in conjunction with WVR statistics tabulated in [1]. We will discuss the effect of normalizing the measurements to a common range distance in Section V.

Figure 14 displays P_c/N_0 versus elevation angle for Ka-band acquired using DSS-54. As this data set includes fewer passes, one can easily see the effects of sampling different range distance such as the "drop" in the upper part of the "envelope" near 39 deg elevation. The P_c/N_0 data plotted in Figure 14 consist of 136327 data points, filtered from ~200000 data points. The P_c/N_0 data were filtered in the same manner as described for DSS-25 (Figure 8).

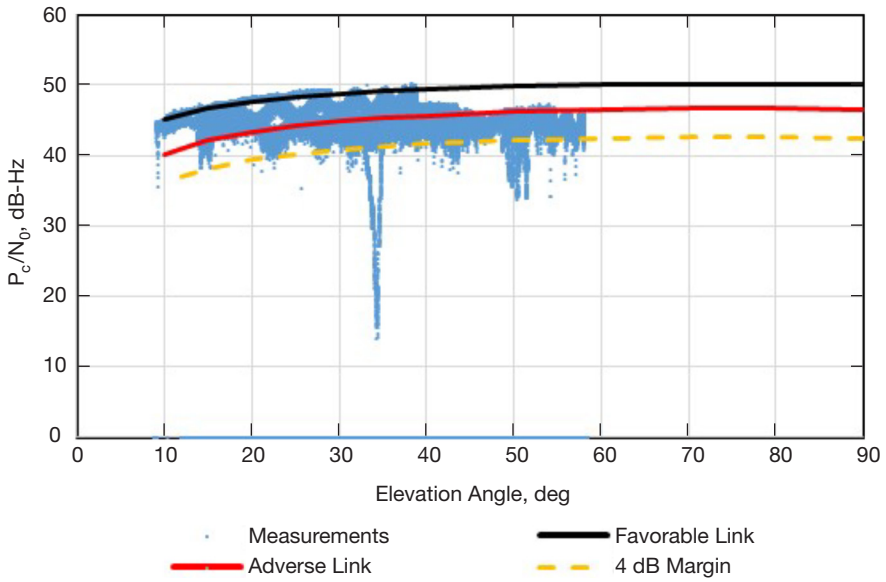

Figure 14. Received P_c/N_0 versus elevation angle for DSS-54 (blue points) with adverse (red) and favorable (black) link curves. Also plotted is the 4-dB margin (relative to adverse) (dashed yellow).

Only one very large fade of ~30 dB magnitude is evident at an elevation angle of ~34 deg. This fade is attributable to weather, as shown by the anti-correlation of P_c/N_0 with SNT (see September 20, 2010, time series in Figure 15). An examination of the AWVR zenith sky temperatures at 31.4 GHz further supports this conclusion (see elevated gray-circle AWVR measurements during the fade period in Figure 15).

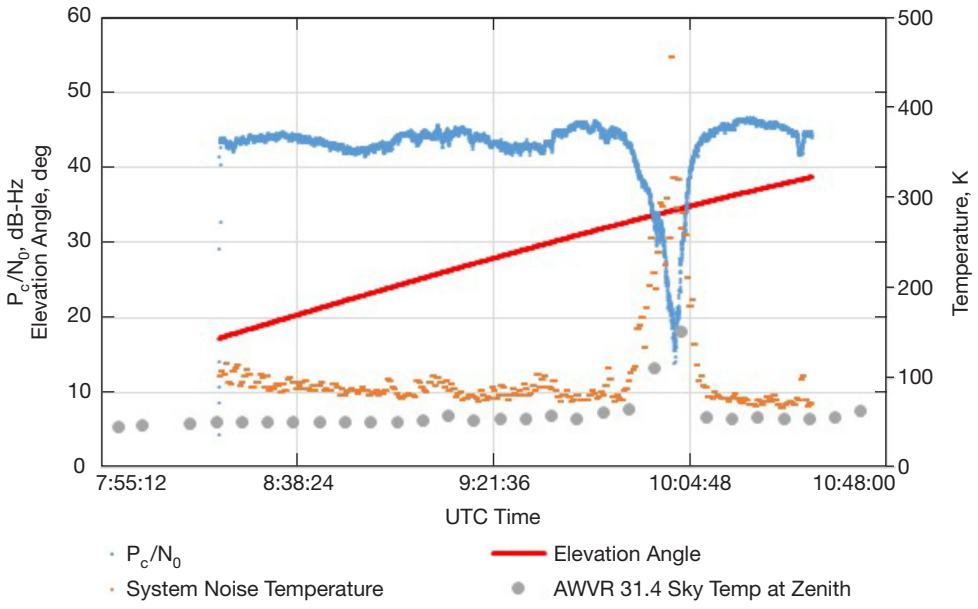

Figure 15. P_c/N_0 and SNT versus time for DSS-54 pass conducted on September 20, 2010, where there is a significant fade feature anti-correlated with a large excursion in SNT. Also shown is AWVR zenith sky temperature at 31.4 GHz.

C. Canberra, Australia

Figure 16 displays the downlink P_c/N_0 versus elevation angle for Ka-band data received at DSS-34 at the DSN tracking site in Canberra, Australia. The favorable link curve does a nice job of tracking the upper envelope bound of the data. Most of the data lie above the 4-dB margin curve. The P_c/N_0 data plotted in Figure 16 consist of 438018 data points, and were filtered from ~540000 initial data points. The data were filtered in the same manner as that described for DSS-25 (Figure 8).

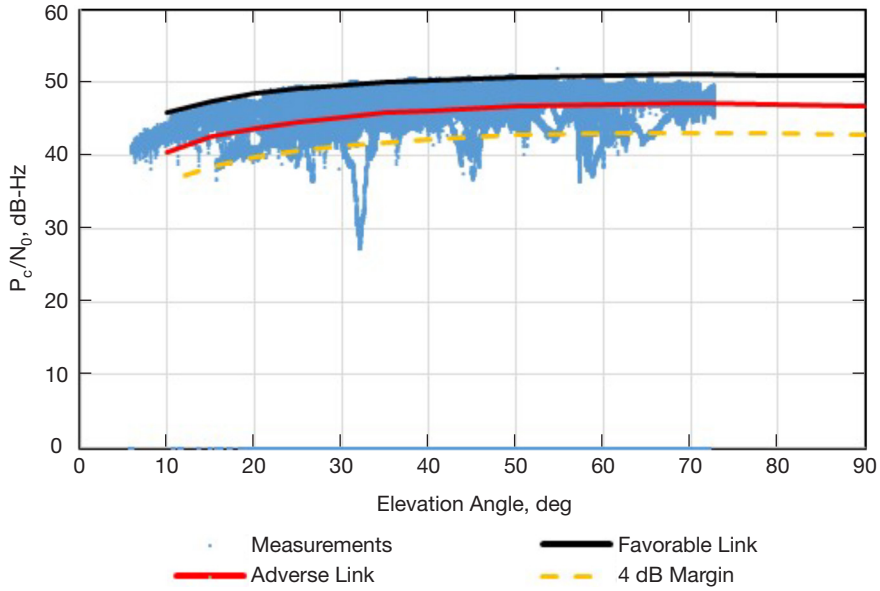

Figure 16. Received P_c/N_0 versus elevation angle for DSS-34 (blue points) with adverse (red) and favorable (black) link curves. Also plotted is the 4-dB margin (relative to adverse) (dashed yellow).

Figure 17 displays the downlink P_c/N_0 versus elevation angle for Ka-band data received at DSS-35 at the Canberra DSN tracking site. The favorable link curve does a reasonably nice job of tracking the upper envelope bound of the data. Almost all the data lie above the 4-dB margin curve. The P_c/N_0 data plotted in Figure 17 consist of 89310 data points, and were filtered from ~122000 initial data points. The data were filtered in the same manner as that described for DSS-25 (Figure 8). It is noted that there are periods of data that lie below the adverse tolerance curve but can be covered by a 4-dB margin (relative to the adverse curve). Some of the data appear to occur during spacecraft roll activities, which includes periodic behavior due to mispointing. However, the peaks of some of the passes appear to coincide with the edge of the favorable link curve, suggesting that spacecraft mispointing is at a minimum during these periods. Given the small number of passes involving the new BWG antenna DSS-35, there are an insufficient number of tracking passes needed in order to capture a wide range of weather effects, contrary to the case of DSS-34 (see Figure 16). The unusual behavior of the P_c/N_0 data at elevation angles below ~13 deg in Figure 17 could be due to ground pickup and/or terrain effects.

Figure 18 displays P_c/N_0 (blue data points) degraded due to weather during a DSS-34 two-way pass conducted on October 8, 2011, along with SNT (brown data points). The anti-correlation between P_c/N_0 and SNT is consistent with atmospheric degradation.

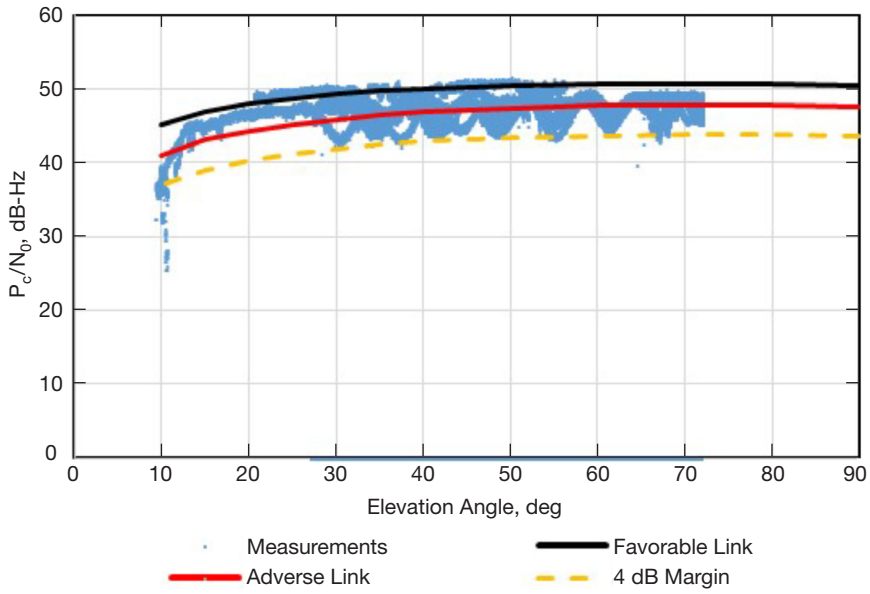

Figure 17. Received P_c/N_0 versus elevation angle for DSS-35 (blue points) with adverse (red) and favorable (black) link curves. Also plotted is the 4-dB margin (relative to adverse) (dashed yellow).

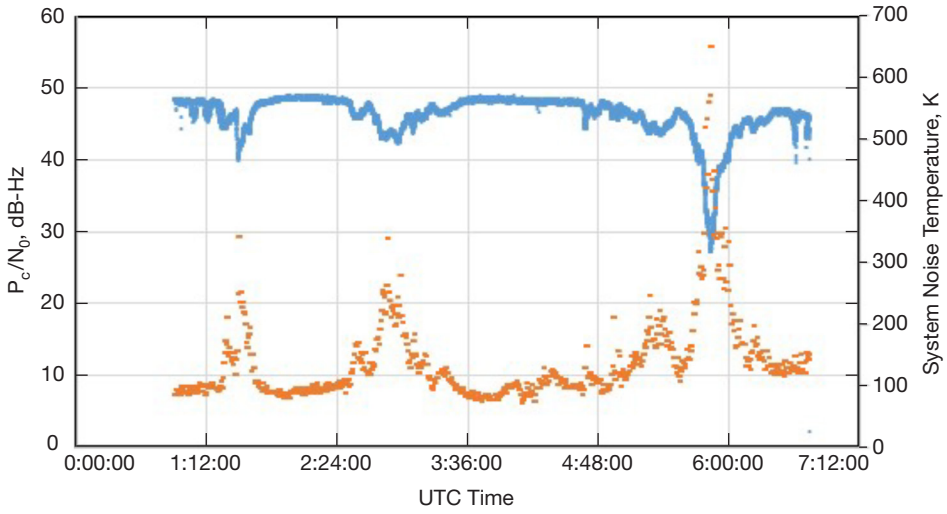

Figure 18. Example of P_c/N_0 (blue data points) degraded due to weather taken at DSS-34 two-way on October 8, 2011, along with SNT (brown data points).

V. Recommended Margin Policy

This section will discuss recommendations for projects with regard to Ka-band margin policy and thresholds. We have focused on the adverse link curves providing a boundary from which we can inspect P_c/N_0 data lying below them. We selected a 4-dB margin curve lying below the adverse link curve to allow us to determine the fraction of the acquired data that lie below it for each tracking site.

Table 1 displays the overall results for each tracking station involved as well as the totals for each tracking site. Over 2 million individual P_c/N_0 measurements from all three tracking sites were used to evaluate statistics due to atmospheric effects. From 187 tracking passes (out of ~250), data were used in the statistical characterization presented in Table 1. The majority of the ~63 tracking passes removed from the statistical characterization were solar conjunction passes where charged-particle degradation was significant or dominant at low solar elongation angles.

Table 1. Overall results for each tracking station and totals for each tracking site.

DSS Number and Location	Number of Passes	Mode	Number of Observations	Number of Observations >4-dB Curve	Percent Above 4-dB Curve
25	67	All	587434	584895	99.57
26	14	All	143488	143197	99.80
Goldstone	81	Total	730922	728092	99.61
34	35	All	438018	431191	98.44
35	10	All	89310	88539	99.14
Canberra	45	Total	527328	519730	98.56
54	10	All	136327	133073	97.61
55	51	All	696418	657918	94.47
Madrid	61	Total	832745	790991	94.99

Upon examination of Table 1, we find that 99.6 percent of the usable data lie above the 4-dB margin curve for Goldstone, 98.6 percent for Canberra, and near 95 percent for Madrid. We believe the majority of the data points that lie below the 4-dB margin curves are due to weather-related degradation. A smaller percentage of these data lying below the 4-dB margin curve are attributable to spacecraft pointing issues. As there are over 10 years of data from the various stations, we speculate that bad weather occurrences may have been undersampled for Goldstone and Canberra, given the high percentages of data lying above 4-dB margin. This would be relative to Madrid, which has a lower percentage of data points above the 4-dB margin curves where bad weather may have been oversampled. However, for all three sites, 95 percent or better of the data lie above the 4-dB curve, suggesting that this is a reasonable recommended margin for preflight planning for projects or programs that may consider using Ka-band telecommunications links. We stress the point that this recommended margin is based on the analyses presented here involving Cassini-specific flight experience. Projects may then opt to adjust this margin up or down as they better define their threshold conditions, and gain more understanding of their requirements as their design evolves and their link parameter uncertainties tighten.

If we normalize all the data discussed in this article to a common range distance, we find that the dispersion bands of the data displayed in Figures 8, 9, 11, 14, 16, and 17 are reduced somewhat. Once we redraw the favorable and adverse link curves and perform the same analysis, we find that the percentages of the data lying above the 4-dB curves are a little lower but similar: 98 percent for Goldstone, 97 percent for Canberra, and 94 percent for Madrid. Here we believe that these results are somewhat more conservative than the results shown in Table 1 as they include some additional data points hindered more by mispointing than by atmosphere.

VI. Conclusions

We examined over 10 years of Cassini closed-loop received Ka-band carrier-level data acquired at all three DSN tracking sites, in order to characterize link performance over a wide range of weather conditions and as a function of elevation angle. Based on this analysis, we have derived a recommendation for a Ka-band link margin that flight projects can utilize in their preflight planning. Here we recommend a threshold assumption of 90 percent weather using statistics tabulated in [1] for the link budget weather parameters, and a margin of 4 dB to cover perceived increased uncertainties at the 32 GHz Ka-band link frequency. We find that a 4-dB margin will ensure a ~94 percent data return at a minimum 20-deg elevation angle under 90 percent weather conditions at 32-GHz Ka-band.

Acknowledgments

We thank Barry Geldzahler, Faramaz Davarian, and Kar-Ming Cheung for their support of this work. We also thank the Cassini Radio Science Team for their support in providing the data sets. We thank Connie Dang of DSN Operations for providing weather data support. We also would like to thank Peter Kinman and Kar-Ming Cheung for valuable review comments.

References

[1] S. D. Slobin, "Atmospheric and Environmental Effects," *DSN Telecommunications Link Design Handbook*, DSN No. 810-005, Space Link Interfaces, Module 105, Rev. D, Jet Propulsion Laboratory, Pasadena, California, September 15, 2009. http://deepspace.jpl.nasa.gov/dsndocs/810-005/105/105D.pdf

[2] P. W. Kinman, "34-m and 70-m Telemetry Reception," *DSN Telecommunications Link Design Handbook*, DSN No. 810-005, Space Link Interfaces, Module 10, Rev. A, Jet Propulsion Laboratory, Pasadena, California, June 13, 2003. http://deepspace.jpl.nasa.gov/dsndocs/810-005/207/207A.pdf

[3] J. H. Yuen, editor, *Deep Space Telecommunications System Engineering*, National Aeronautics and Space Administration, Washington, DC, July 1982; reprinted by Plenum Press, New York, 1982.

[4] J. H. Yuen, "Deep Space Communications: An Introduction," in *Deep Space Communications*, First Edition, Jim Taylor, editor, John Wiley and Sons, Inc., 2016.

[5] R. Ludwig and J. Taylor, "Voyager Telecommunications," in *Deep Space Communications*, First Edition, Jim Taylor, editor, John Wiley and Sons, Inc., 2016.

[6] J. Taylor, A. Makovsky, A. Barbieri, R. Tung, P. Estabrook, and A. G. Thomas, *Mars Exploration Rover Telecommunications*, DESCANSO Design and Performance Summary Series. http://descanso.jpl.nasa.gov/DPSummary/MER_article_cmp20051028.pdf

[7] T. Pham and J. Liao, "Performance Analysis of Operational Ka-band Link with Kepler," *Proceedings of SPACOMM 2016, The Eighth International Conferences on Advances in Satellite and Space Communications*, Lisbon, Portugal, International Academy, Research and Industry Association (IARIA), February 21–25, 2016.

[8] D. Morabito, L. Wu, and S. Slobin, "Weather Forecasting for Ka-band Operations: Initial Study Results," *The Interplanetary Network Progress Report*, vol. 42-206, Jet Propulsion Laboratory, Pasadena, California, pp. 1–24, August 15, 2016. http://ipnpr.jpl.nasa.gov/progress_report/42-206/206C.pdf

[9] A. Kliore, J. Anderson, J. Armstrong, S. Asmar, C. Hamilton, et al., "Cassini Radio Science," *Space Science Reviews*, vol. 115, no. 1–4, 14 pp. 1–70, 2004.

[10] S. D. Slobin, "34-m BWG Stations Telecommunications Interfaces," *DSN Telecommunications Link Design Handbook*, DSN No. 810-005, Space Link Interfaces, Module 104, Rev. H, Jet Propulsion Laboratory, Pasadena, California, August 1, 2015. http://deepspace.jpl.nasa.gov/dsndocs/810-005/104/104H.pdf

[11] D. Morabito and R. Hastrup, "Communications with Mars During Periods of Solar Conjunction: Initial Study Results," *The Interplanetary Network Progress Report*, vol. 42-147, Jet Propulsion Laboratory, Pasadena, California, July–September 2001, pp. 1–16, November 15, 2001. http://ipnpr.jpl.nasa.gov/progress_report/42-147/147C.pdf